

# VERIFICATION AND APPLICATION OF SuperMC3.3 TO LEAD-BISMUTH-COOLED FAST REACTOR

by

**Hui DING**<sup>1,2</sup>, **Quan GAN**<sup>1</sup>, **Lijuan HAO**<sup>1,\*,\*\*</sup>, **Jing SONG**<sup>1</sup>, and **Yican WU**<sup>1</sup>

<sup>1</sup>Key Laboratory of Neutronics and Radiation Safety,  
Institute of Nuclear Energy Safety Technology, Chinese Academy of Sciences, Hefei, Anhui, China  
<sup>2</sup>University of Science and Technology of China, Hefei, Anhui, China

Scientific paper

<https://doi.org/10.2298/NTRP190220015D>

Lead-cooled fast reactors have multilayered designs and large internal temperature differences, which cause challenges in simulating reactor physics. SuperMC, a large-scale integrated software system for neutronics design, is inherently able to address complex geometries and multi-temperature problems. The purpose of this study is to verify the applicability of SuperMC to the lead-bismuth-cooled fast reactor RBEC-M. The multi-temperature cross-section generation function of SuperMC was employed and showed good performance. Based on the ENDF/B-VII.1 library, the effective multiplication factor  $k_{\text{eff}}$  obtained by SuperMC showed good agreement with those from previous works. The relationship of  $k_{\text{eff}}$  and  $^{15}\text{N}$  enrichment applied to the fuel material was also studied, with the results showing that increased  $^{15}\text{N}$  could significantly improve  $k_{\text{eff}}$ . The axial power profile and kinetics parameters for the benchmark were then calculated and analyzed. This work thus verified the applicability of SuperMC for comprehensive neutronics simulations for lead-bismuth-cooled fast reactors.

*Key words:* RBEC-M, fast reactor, lead-bismuth-cooled reactor, SuperMC, reactor kinetics, reactor physics

## INTRODUCTION

Lead-cooled fast reactors (LFR) are among the most promising advanced Generation IV nuclear systems for demonstration and commercialization [1, 2]. They show the advantages of robust fuel cycling and good safety performance, as well as new physical characteristics. Molten lead and lead-bismuth mixtures, as the primary coolants of LFR, have low neutron absorption. LFR operate with fast neutron spectra because the neutrons are not slowed as efficiently during interaction with heavy nuclides. In addition, LFR have high operating temperatures of  $>500$  °C. These special features require the performance of comprehensive neutronics simulations. Some neutronics analyses of LFR, such as BREST-OD-300 [3] and the European Lead-Cooled Training Reactor (ELECTRA) [4], have been reported previously. In this work, the simulation of the lead-bismuth-cooled reactor RBEC-M is performed. The RBEC-M is a distinctive reactor including three core regions with lead-bismuth coolants, mixed nitride fuels,

and multi-temperature distributions [5]. This simulation was performed using SuperMulti-functional Calculation Program for Nuclear Design and Safety Evaluation (SuperMC) to verify the applicability of SuperMC to the RBEC-M.

SuperMC [6-8], developed by the FDS Team, is a large-scale integrated software system for neutronics design. The system adopts the Monte Carlo method for neutron transport analysis. It has contributed significantly to many research fields, including materials development [9-12], the innovative design of advanced reactors [13,14], and neutronics experiments [15, 16]. The verification and validation of SuperMC for nuclear criticality safety and shielding benchmark suites were systematically performed previously [17, 18]. SuperMC has powerful 3-D geometric modeling capabilities, supporting the creation and editing of geometric shapes such as cuboids, cylinders, and spheres. SuperMC's hierarchical modeling can facilitate quick and accurate construction of complete reactor models, which has been applied to some fission reactor cores [19]. The latest version, SuperMC3.3, supports multi-temperature on-the-fly (OTF) functions and can

\* Corresponding author; e-mail: [lijuan.hao@fds.org.cn](mailto:lijuan.hao@fds.org.cn)

\*\* P.O. Box 1135, No. 350, Shushanhu Road, Hefei, Anhui, China

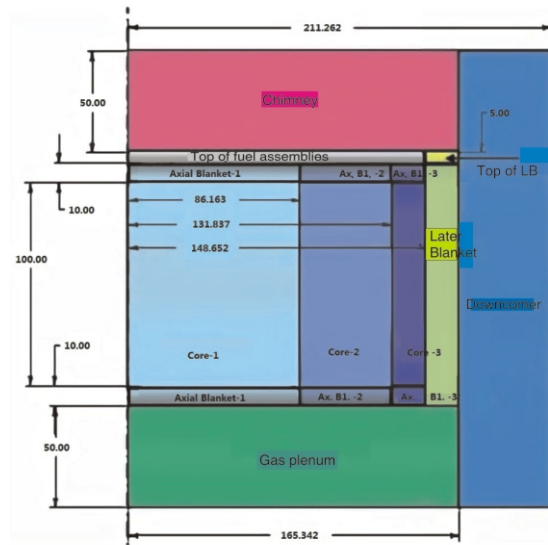
generate cross-sections of multiple temperatures to meet the demands of large temperature variations in some fission reactors.

In this paper, the modeling process of the International Atomic Energy Agency (IAEA) RBEC-M benchmark in SuperMC was first described. Then the neutronics calculations were carried out using SuperMC, and the results were analyzed and discussed.

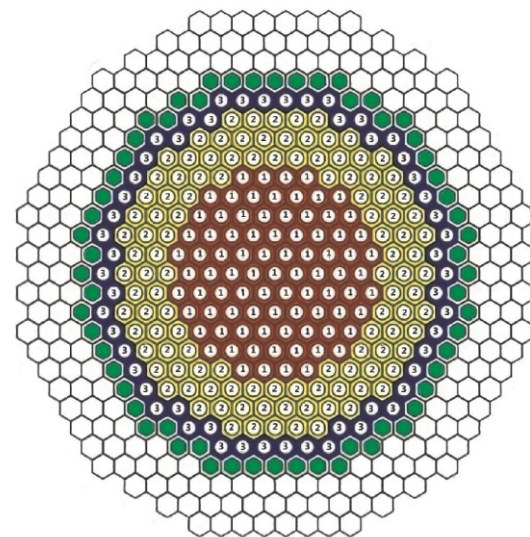
### DESCRIPTION OF THE BENCHMARK

The IAEA benchmark problem [20] was derived from the 900 MWt RBEC-M reactor core design, proposed by the Russia Research Center *Kurchatov Institute* (RRC KI). Reactor solutions, including hexagonal fuel assemblies (FA), lateral and axial blankets, wide fuel rod lattices, and high  $^{15}\text{N}$  enrichment, facilitate improvement of breeding parameters and reactivity effects [21]. The R-Z model with dimensional parameters (in centimeters) of the RBEC-M benchmark is shown in fig. 1(a); the homogenized model comprises fifteen physical zones, including three core zones. The core zones have 253 FA which are divided into three parts based on fuel volume fractions. The configuration of the RBEC-M core is provided in fig. 1(b).

Mixed uranium-plutonium nitride fuel ( $\text{U}_{0.863} + \text{Pu}_{0.137}\text{N}$ ) is applied in all core zones; the cladding and the structural material are ferritic/martensitic stainless steel (12 % Cr-Si). The periphery of the core is surrounded by radial blankets of 10 cm in height and lateral blankets comprising pellets of depleted uranium nitride. The upper and lower ends of the reactor are a 50-cm-tall chimney and a gas plenum, respectively. In addition, the downcomer channel for coolant circulation is located at the outer side. For each physical zone, the component-wise temperatures (in kelvins) of elements are summarized in tab. 1. Detailed nuclide densities (in 1/barn-cm) are given in Ref [20].



(a) The R-Z reactor model



(b) Core assembly model

Figure 1. Benchmark model of RBEC-M core

Table 1. Temperatures [K] of physical zones of the RBEC-M reactor

Physical zone	Fuel	Steel	Coolant
Core-1	1200	800	700
Core-2	1100	800	700
Core-3	1000	800	700
Axial blanket of Core-1	900/700*	800/600*	800/600*
Axial blanket of Core-2	900/700*	800/600*	800/600*
Axial blanket of Core-3	900/700*	800/600*	800/600*
Lateral blanket	700	600	600
Top of fuel assemblies		600	800
Gas plenum		600	600
Top of assemblies of lateral blanket		600	600
Downcomer		700	700
Chimney		800	800

\* Temperatures in top/bottom of the physical zones

## SIMULATION METHODS

### Modeling

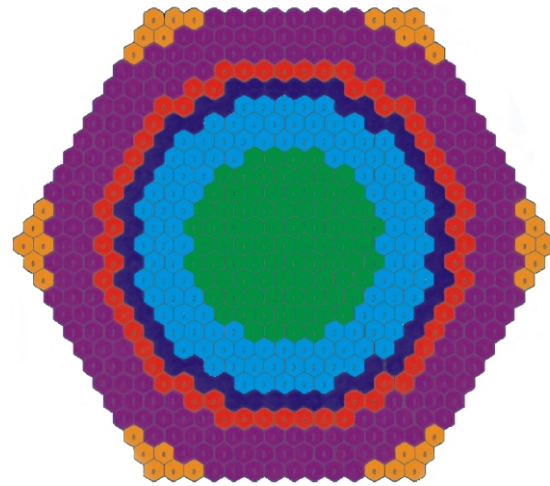
The computer-aided design (CAD)-based modeling built into SuperMC enables convenient and accurate construction of the reactor model. Geometric entities can be created and edited via a graphical user interface (GUI). Moreover, hierarchical geometric functionality allows modular and efficient modeling by the establishment of geometric relationships, such as similarity and filling, of a reactor model. With this method, the RBEC-M benchmark geometric model should be divided into three layers. Thirteen homogenization regions (with the three core zones treated as one region) are considered as the upper layer; the three core zones and lateral blanket are filled with different FA in a hexagonal lattice. The core assembly in fig. 2(a) shows the middle layer; the figure depicts that the horizontal layout of core exhibits different core areas. The fill geometry in each assembly is the bottom layer. Figure 2(b) shows a quarter of the entire reactor model.

### Multi-temperature online processing

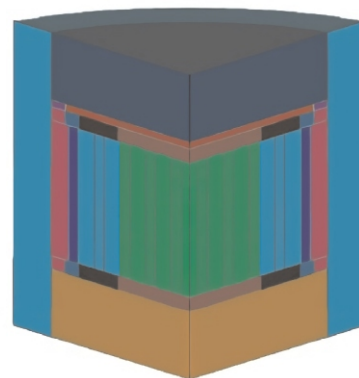
To satisfactorily model the temperature range throughout all physical zones of RBEC-M benchmark, the nuclear cross-sections at seven temperatures (600, 700, 800, 900, 1000, 1100, and 1200 K) should be obtained. Current released nuclear databases cannot handle the multi-temperature characteristics of the benchmark. In such a case, we can employ a nuclear data processing code, such as NJOY, to process the nuclear data files and pre-generate the libraries covering the required temperatures. This method is offline with the disadvantages of high memory and time consumption [22]. SuperMC's multi-temperature OTF function with a novel Doppler broadening method [23] enables the online analysis of temperature distributions of the model and generation of corresponding cross-sections, and no extra memory is required in neutron transport calculations. Its implementation in SuperMC3.3 is shown in fig. 3. This function was used to produce the multi-temperature library based on the ENDF/B-VII.1 according to the real temperature of each region.

## RESULTS AND DISCUSSION

This work employs SuperMC to evaluate the criticality performance of RBEC-M, including the effective multiplication factor  $k_{\text{eff}}$ , axial power distribution, and kinetics parameters. To perform criticality calculations, the source is defined as 30000 particles per cycle for 500 cycles with the 50 initial cycles



(a) The core assembly



(b) 1/4 reactor model

**Figure 2. Geometric model of RBEC-M**

skipped by the source-modeling module of SuperMC. The computing platform is an Intel Xeon E5-2650 server with 20 cores. The online generation function is verified in the effective multiplication factor calculation, and subsequent simulation is performed based on that function.

### Effective multiplication factor

Based on the ENDF/B-VII.1 library, the  $k_{\text{eff}}$  calculation results with SuperMC and available results in the IAEA report [20] for the RBEC-M reactor benchmark are provided in tab. 2.

As shown in tab. 2, in this calculation, the  $k_{\text{eff}}$  results are fully accepted for SuperMC compared with other codes. The discrepancies in  $k_{\text{eff}}$  among these codes are relatively large, and it can be inferred that different libraries significantly affect the reactions of some key nuclides [24], such as  $^{208}\text{Pb}$ ,  $^{238}\text{U}$ , and  $^{239}\text{Pu}$ . Library data pre-processing could also cause the discrepancy. In this work, the results calculated with the library produced by NJOY and by the SuperMC OTF

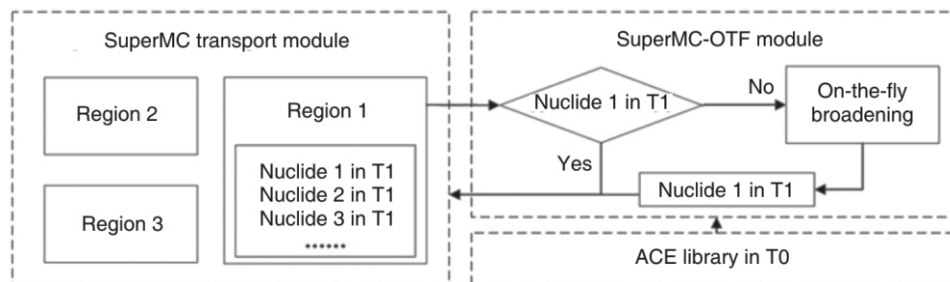


Figure 3. Flowchart of SuperMC-OFF

Table 2. The  $k_{eff}$  calculations with different codes

Code	Library	$k_{eff}$
SuperMC	ENDF/B-VII.1 with OTF	1.00049 0.00011
SuperMC	ENDF/B-VII.1 with NJOY	1.00025 0.00012
Gidropress/KINRZ	ENDF/B-VI	1.0084
RRC KI/MCNP-5	ENDF/B-VI	1.00375
RRC KI/MCNP-5	ENDF/B-VII	0.99514
ANL/TWODANT	ENDF/B-V.2	0.99937

function were compared. The relative difference  $\Delta k_{eff}$  was calculated with the equation

$$\Delta k_{eff} = \frac{k_{eff}^{NJOY}}{k_{eff}^{SuperMC\ OTF}} - 1 \quad (1)$$

$$\sigma = \sqrt{(\sigma^{NJOY})^2 + (\sigma^{SuperMC\ OTF})^2} \quad (2)$$

It can be obtained that  $\Delta k_{eff} = -0.024\%$  and  $\sigma = 0.016\%$ . The  $\Delta k_{eff}$  result was within a  $3\sigma$  interval [25], which proves the accuracy of the SuperMC-OFF. To further evaluate the performance of SuperMC-OFF, the calculation times with the two methods are provided in tab. 3.

It can be seen from the table that the SuperMC-OFF cross-section generation method is nearly equivalent in efficiency to the transport calculation using the broadened cross-section by NJOY. The broadening time results show that the cross-section broadening efficiency, using the SuperMC-OFF, is more than 100 times that of NJOY. Accordingly, the OTF cross-section generation in SuperMC is an effective, pre-processing method and is used for the rest of the calculations.

In LFR design, a higher  $k_{eff}$  corresponds to a lower power grade of Pu enrichment in the fuel, which indicates greater economy in fuel loading [26]. The  $k_{eff}$  performance is affected (more or less) by fractions of key nuclides in the core region [27]. Some studies have investigated the relationship between  $k_{eff}$  and  $^{208}\text{Pb}$  [25, 26] in coolant. Higher  $^{15}\text{N}$  enrichment of

Table 3. Performance of calculation with SuperMC-OFF and NJOY

Method	Transport calculation time [s]	Broadening time [s]
SuperMC-OFF	2968.2	15.303
NJOY	2926.2	2074.1

nitride fuel material has been applied to RBEC-M reactors to improve  $k_{eff}$  performance. Nitrogen is used with 99.9% enrichment of  $^{15}\text{N}$ , while  $^{15}\text{N}$  in nature has the enrichment of only 0.4%. However, a corresponding numerical analysis has not yet been provided. In order to study the effect of high  $^{15}\text{N}$  enrichment on  $k_{eff}$ , 11 different fractions of  $^{15}\text{N}$  were simulated; the results are as plotted in fig. 4.

As the  $^{15}\text{N}$  fraction increases, the  $k_{eff}$  value is increased, with a nearly linear relationship from 10% to 90%. For every 10% increase in the  $^{15}\text{N}$  enrichment, the  $k_{eff}$  value is increased by about 290 pcm (per cent mille,  $10^{-5}$ ). The application of  $^{15}\text{N}$  thus substantially improves the  $k_{eff}$ . When the fraction of  $^{15}\text{N}$  is >90%, the improvement is limited. Compared with the 99.9% enrichment in the benchmark, the  $k_{eff}$  value is only decreased by 6.6 pcm when the enrichment is reduced to 99%. Because 99% enrichment of  $^{15}\text{N}$  is more easily achieved than 99.9% [28], using 99% enrichment of  $^{15}\text{N}$  is recommended as it has little effect on  $k_{eff}$ , as well as a lower cost.

### Axial power profile

The axial core power profile is an important reference factor for nuclear engineers to control reactors. The power distribution, calculated using SuperMC code, is a normalized result; to obtain an absolute value that can be compared, the tally results must be multiplied by the source strength factor –  $Q$ , which is estimated by the equation

$$Q = \frac{\text{Power}}{E} N \quad (3)$$

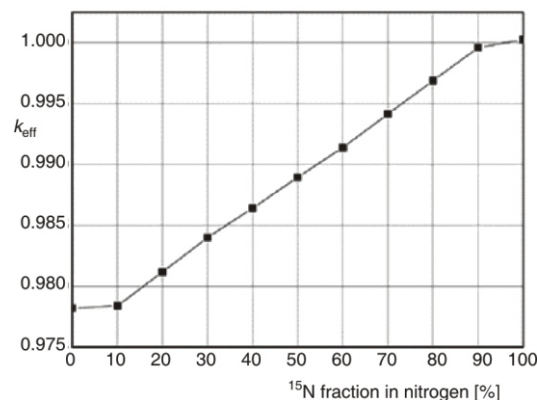
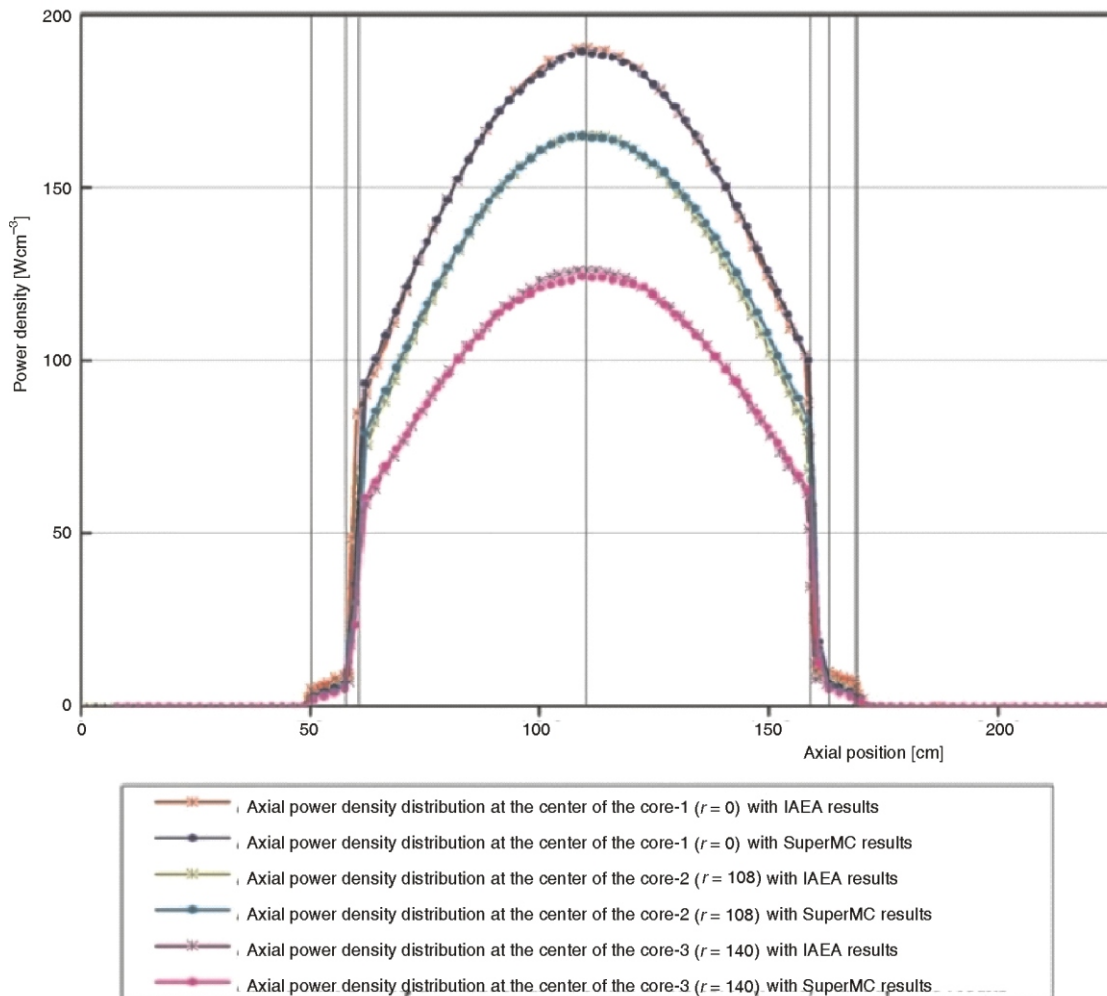


Figure 4. The  $k_{eff}$  with respect to the original design in the benchmark



**Figure 5. The RBEC-M axial power distribution**

where  $E$  represents the thermal fission energy and  $N$  is the number of neutrons produced per fission. Many fission nuclides are present in the benchmark with the following thermal fission energies obtained from the ENDF/B-VII.1 library [29]: 201.46 0.10 MeV for  $^{235}\text{U}$ , 208.51 0.17 MeV for  $^{238}\text{U}$ , 200.92 0.24 MeV for  $^{238}\text{Pu}$ , 204.76 0.14 MeV for  $^{239}\text{Pu}$ , 213.63 0.23 MeV for  $^{240}\text{Pu}$ , 216.11 0.23 MeV for  $^{241}\text{Pu}$ , 218.20 1.133 MeV for  $^{242}\text{Pu}$ , and 214.78 0.24 MeV for  $^{241}\text{Am}$ . Therefore, using the thermal fission energy will cause discrepancies in the power value, especially for the power peak, among different calculations. In this research, the weighted fission energy 207 MeV was used according to the fission rates in the various isotopes.

Figure 5 depicts the axial core power profile, which is determined at the center of each core zone. The power distribution calculated with SuperMC is in good agreement with the IAEA results. With the midplane of the core as the axis, the power distribution on the left and right side is almost symmetrical. On the left side, the transitions of every curve are near the material boundaries. A sudden change in power occurs between the gas plenum and blankets, with a sharp

climb in power between the blankets and core zones. Because of the symmetry of the three core zones, the power distribution is parabolic in these regions with the power peak appearing in the midplane of the core. Under careful observation, some slight differences appear between the lower and upper boundary of the core. Unlike the lower boundary, the upper boundary includes FA tops, which could reduce the neutron leakage. Therefore, the power near the core upper boundary is higher than that at the lower boundary.

### Reactor kinetics parameters

Reactor kinetics parameters, such as the effective delayed neutron fraction  $\beta_{\text{eff}}$  and the neutron generation time  $\Lambda$ , are physical parameters of great relevance to the reactor safety operation. Higher  $\beta_{\text{eff}}$  and  $\Lambda$  can substantially improve the kinetic response of the reactor. Table 4 shows the results for these parameters obtained by SuperMC and RRC KI [30]. Typical parameters [31] for fast reactors are also given in the table.

Although the numerical precisions are different, both kinetics parameters obtained by SuperMC are

**Table 4. SuperMC and RRC KI kinetics parameters results compared to those of typical fast reactors**

	$\beta_{\text{eff}}$	$\Lambda(\text{s})$
SuperMC	$3.66 \times 10^{-3}$	$4.53 \times 10^{-7}$
RRC KI	$3.7 \times 10^{-3}$	$4.5 \times 10^{-7}$
Typical parameters in fast reactors	$3.32 \times 10^{-3}$	$5 \times 10^{-7}$

consistent with the RRC KI results. As shown in the table, the RBEC-M reactor exhibits a slightly higher delayed neutron fraction than typical fast reactors. Considering the delayed neutrons, the average lifetime of fission neutrons  $l$  is defined by

$$l = \beta_{\text{eff}} \Lambda \quad (4)$$

Because  $\beta_{\text{eff}}$  is much larger than  $\Lambda$ ,  $l$  depends mainly on  $\beta_{\text{eff}}$ . In the RBEC-M reactor, the larger  $\beta_{\text{eff}}$  implies a longer average time interval between two generations of neutrons, thereby delaying changes in neutron density. This yields a slower power excursion when introducing the same reactivity jump.

## CONCLUSIONS

Advanced LFR show new neutronics characteristics. In this work, the lead-bismuth RBEC-M reactor was used to verify the advanced reactor physics code SuperMC. Modeling, calculation, and visualization were all performed using SuperMC.

Compared with the IAEA report on the RBEC-M reactor, good consistencies were achieved for  $k_{\text{eff}}$  and power profile. Based on the ENDF/B-VII.1 library, the relative difference of  $k_{\text{eff}}$  as calculated with the library produced by NJOY and by the SuperMC-OTF function was within a  $3\sigma$  interval. The calculation results also showed that SuperMC-OTF broadening efficiency is more than 100 times that of NJOY. In addition, the  $k_{\text{eff}}$  effect of  $^{15}\text{N}$  application was analyzed; increased  $^{15}\text{N}$  showed beneficial improvements in  $k_{\text{eff}}$  performance. Reactor kinetics parameters of the effective delayed neutron fraction  $\beta_{\text{eff}}$  and the neutron generation time  $\Lambda$  were calculated and compared with those of typical fast reactors to reflect the kinetic response performance of the RBEC-M.

In this work, hierarchical modeling and online cross-section generation in SuperMC yielded great efficiency improvements in reactor simulation. In the future, fuel burnup analysis of the RBEC-M benchmark will be performed with SuperMC.

## ACKNOWLEDGMENT

This work was supported by the National Key R&A Program of China (2018YFB1900601), the Strategic Priority Research Program of Chinese Academy of Sciences (Grand No. XDA22010504), the Ker Research Program of the Chinese Academy of Sci-

ences (Grand No. ZDRW-KT-2019-1-0202), the project of HIPS (KP-2017-19), the project of Chinese Academy of Sciences (XXH13506-104). Young Elite Scientists Sponsorship Program by CAST (2017QNRC001).

## AUTHORS' CONTRIBUTIONS

The modeling and calculations using SuperMC were performed by H. Ding. The manuscript and the figures were prepared by H. Ding and were revised by Q. Gan and L. Hao. All the authors contributed to the development and the use of SuperMC code, including analysis and discussion of the results.

## REFERENCES

- [1] Wu, Y., *et al.*, Development Strategy and Conceptual Design of China Lead Based Research Reactor, *Annals of Nuclear Energy*, 87 (2016), Part 2, pp. 511-516
- [2] Wu, Y., Design and R&D Progress of China Lead-Based Reactor for ADS Research Facility, *Engineering*, 2 (2016), 1, pp. 124-131
- [3] Koltashev, D. A., Stakhanova, A. A., Neutronics Calculation of Fast Reactors by the EUCLID/V1 Integrated Code, *Journal of Physics: Conference Series*, 781 (2017), 1, 012003
- [4] Wolniewicz, P., *et al.*, Detecting Neutron Spectrum Perturbations Due to Coolant Density Changes in a Small Lead-cooled Fast Nuclear Reactor, *Annals of Nuclear Energy*, 1 (2013), 58, pp. 102-109
- [5] Mikityuk, K., *et al.*, RBEC-M Lead-Bismuth Cooled Fast Reactor: Optimization of Conceptual Decisions. *Proceeding, 10<sup>th</sup> International Conference on Nuclear Engineering*, Arlington, Va., USA, 14-18 April 2007
- [6] Wu, Y., Multi-Functional Neutronics Calculation Methodology and Program for Nuclear Design and Radiation Safety Evaluation, *Fusion Science and Technology*, 74 (2018), 4, pp. 321-329
- [7] Wu, Y., FDS Team, CAD-Based Interface Programs for Fusion Neutron Transport Simulation, *Fusion Engineering and Design*, 84 (2009), 7-11, pp. 1987-1992
- [8] Wu, Y., *et al.*, CAD-Based Monte Carlo Program for Integrated Simulation of Nuclear System SuperMC, *Annals of Nuclear Energy*, 82 (2015), Aug., pp. 161-168
- [9] Huang, Q., *et al.*, Recent Progress of R&D Activities on Reduced Activation Ferritic/Martensitic Steels, *Journal of Nuclear Materials*, 442 (2013), 1-3, pp. S2-S8
- [10] Huang, Q., *et al.*, Progress in Development of China Low Activation Martensitic Steel for Fusion Application, *Journal of Nuclear Materials*, 367 (2007), Part A, pp. 142-146
- [11] Huang, Q., Status and Improvement of CLAM for Nuclear Application, *Nuclear Fusion*, 57 (2017), 8, 086042
- [12] Wu, Y., Design Status and Development Strategy of China Liquid Lithium-Lead Blankets and Related Material Technology, *Journal of Nuclear Materials*, 367 (2007), Part B, pp. 1410-1415
- [13] Wu, Y., *et al.*, Identification of Safety Gaps for Fusion Demonstration Reactors, *Nature Energy*, 1 (2016), 12, 16154

- [14] Wu, Y., FDS Team, Conceptual Design of the China Fusion Power Plant FDS-II, *Fusion Engineering and Design*, 83 (2008), 10-12, pp. 1683-1689
- [15] Wu, Y., et al., FDS Team, A Fusion-Driven Subcritical System Concept Based on Viable Technologies, *Nuclear Fusion*, 51 (2011), 10, 103036
- [16] Wu, Y., et al., Development of High Intensity D-T Fusion Neutron Generator HINEG, *International Journal of Energy Research*, 42 (2018), 1, pp. 68-72
- [17] Zhang, B., et al., Criticality Validation of SuperMC with ICSBE, *Annals of Nuclear Energy*, 87 (2016), Jan., pp. 494-499
- [18] Chen, C., et al., FDS Team, Validation of Shielding Analysis Capability of SuperMC with SINBAD, *EPJ Web of Conferences*, 153 (2017), Sept., 02009
- [19] Gan, Q., et al., CAD-Based Hierarchical Geometry Conversion Method for Modeling of Fission Reactor Cores, *Annals of Nuclear Energy*, 94 (2016), Aug., pp. 369-375
- [20] Sienicki, J. J., et al., Status Report on the Small Secure Transportable Autonomous Reactor (SSTAR)/Lead-Cooled Fast Reactor (LFR) and Supporting Research and Development, Lemont, Ill., Argonne National Lab, USA, 2016
- [21] Bakir, G., Yapici, H., Analysis of Fuel Rejuvenation Times in a Fusion Breeder Reactor Fuelled with a Mixture of Uranium-Thorium Oxides for the CANDU Reactor, *Nucl Technol Radiat*, 32 (2017), 3, pp. 193-203
- [22] Yesilyurt, G., et al., On-The-Fly Doppler Broadening for Monte Carlo Codes, *Nuclear Science and Engineering*, 171 (2012), 3, pp. 239-257
- [23] Chen, R., et al., On-The-Fly Doppler Broadening Method Based on Optimal Double-Exponential Formula, *Nuclear Science and Techniques*, 28 (2017), 11, 166
- [24] Milošević, M., et al., Effects of Lead Cross Section Uncertainties on the RBEC-M Fast Reactor Benchmark Results, *Proceedings*, 52<sup>nd</sup> ETRAN Conference, Palić, Serbia, June 8-12, 2008
- [25] Jaboulay, J.-C., et al., TRIPOLI-4® Monte Carlo Code ITER A-lite Neutronic Model Validation, *Fusion Engineering and Design*, 89 (2014), 9-10, pp. 2174-2178
- [26] Khorasanov, G. L., Blokhin, A. I., Benefits in Using Lead-208 Coolant for Fast Reactors and Accelerator Driven Systems. Current Research in Nuclear Reactor Technology in Brazil and Worldwide, IntechOpen, London, United Kingdom, 2013, pp. 194-208
- [27] Mirghaffari, R., et al., Neutronic Simulation of a CANDU-6 Reactor with Heavy Water-Based Nanofluid Coolant, *Nucl Technol Radiat*, 32 (2017), 4, pp. 320-326
- [28] Ding, X. C., et al., High Enrichment of <sup>15</sup>N Isotope by Ion Exchange for Nitride Fuel Development, *Progress in Nuclear Energy*, 50 (2007), 2-6, pp. 504-509
- [29] Chadwick, M. B., et al., ENDF/B-VII.1 Nuclear Data for Science and Technology: Cross Sections, Covariances, Fission Product Yields and Decay Data, *Nuclear Data Sheets*, 112 (2011), 12, pp. 2887-2996
- [30] Mikityuk, K., Safety Parameters of Advanced RBEC-M Lead-Bismuth Cooled Fast Reactor, *Proceedings*, PHYSOR-2002, Seoul, Korea, 7-10 October 2002
- [31] Kodeli, I.-A., et al., Uncertainty Analysis of Kinetic Parameters for Design, Operation and Safety Analysis of SFR, *Proceedings*, International Conference on Fast Reactors and Related Fuel Cycles: Next Generation Nuclear Systems for Sustainable Development (FR17), IAEA-CN-245-136, Yekaterinburg, Russia, 26-29 June 2017

Received on February 20, 2019

Accepted on April 22, 2019

Хуеј ДИНГ, Ђуен ГАН, Лиђуен ХАО, Ђинг СУНГ, Јицан ВУ

## ВЕРИФИКАЦИЈА И ПРИМЕНА SuperMC3.3 ПРОГРАМСКОГ СИСТЕМА НА БРЗИ РЕАКТОР ХЛАЂЕН ОЛОВОМ И БИЗМУТОМ

Брзи реактори хлађени оловом имају вишеслојне структуре и велике унутрашње температурне разлике, што представља изазове за симулацију физичких процеса реактора. SuperMC, велики интегрисани софтверски систем за прорачун неутрона, изворно је способан да реши сложене геометрије и проблеме са вишеструком температуром. Сврха овог рада је да провери применљивост SuperMC програма на бром реактору RBEC-M хлађеним оловом и бизмутом. Коришћена је функција SuperMC програма за генерисање температурно зависних пресека и при томе је показала добра својства. На основу ENDF/B-VII.1 библиотеке, ефективни фактор умножавања неутрона  $k_{\text{eff}}$  израчунат SuperMC програмом добро се слагао са ефективним факторима из претходних радова. Такође је проучавана и веза између  $k_{\text{eff}}$  и <sup>15</sup>N обогаћивања која је примењена на гориви материјал, а резултати показују да повећање <sup>15</sup>N може значајно побољшати  $k_{\text{eff}}$ . Затим су израчунати и анализирани аксијални профил снаге и кинетички параметри за референтну вредност. Овим радом је тако верификована применљивост SuperMC програма за свеобухватне симулације неутрон брзих реактор хлађених оловом и бизмутом.

Кључне речи: RBEC-M, брзи реактор, реактор хлађен оловом и бизмутом, SuperMC, реакторска кинетика, физика реактора